CORE
Metadata, citation and similar papers at core.ac.uk
Provided by Repository of the Academy's Library

Polyhedron 67 (2014) 481-489

# Two Hydroxypyridinecarboxylic Acid Derivatives as Possible Chelating Agents in Neurodegenerative Diseases: Equilibrium Complexation Studies with Cu(II) and Zn(II).

Éva Sija[a], Nóra Veronika Nagy[b], Valentina Gandin[c], Christine Marzano[c], Tamás Jakusch[d], Annalisa Dean[e], Valerio B. Di Marco[e*], Tamás Kiss[a,d*]

[a]HAS-USZ Bioinorganic Chemistry Research Group, Dóm tér 7. H-6720 Szeged, Hungary

[b]Institute of Molecular Pharmacology, Research Centre for Natural Sciences, HAS
Pusztaszeri út 59-67, H-1025 Budapest, Hungary

[c]Department of Pharmaceutical Sciences, University of Padova, Via Marzolo, 5, 35131 Padova, Italy

[d]Department of Inorganic and Analytical Chemistry, University of Szeged, Dóm tér 7. H-6720 Szeged, Hungary, e-mail: tkiss@chem.u-szeged.hu

[e]Department of Chemical Sciences, University of Padova, via Marzolo 1, 35131 Padova, Italy, e-mail: valerio.dimarco@unipd.it

## Abstract

The complexes formed between 4-hydroxy-5-methyl-3-pyridinecarboxylic acid (DQ5) and 1,5-dimethyl-4-hydroxy-3-pyridinecarboxylic acid (DQ715) and Cu(II) and Zn(II) were investigated in aqueous solution. The proton dissociation constants of the ligands, the stability constants, and the coordination modes of the metal complexes formed were determined by pH-potentiometric, and spectral (UV-vis and EPR or $^1$H NMR) methods. The results show that in the pH range between 2 and 10 mono an bis complex formed through bidentate coordination of the ligands. The biological MTT-test reveals that the DQ715 ligand is able to lower the cytotoxic effect of Cu(II) in human embryonic kidney HEK-293 cells.

## Graphical abstract

The complex formation have been characterized by pH-potentiometric and spectral (UV-vis and EPR and $^1$H NMR) methods between two hydroxy pyridine carboxylic acids and Cu(II) and Zn(II) ions.

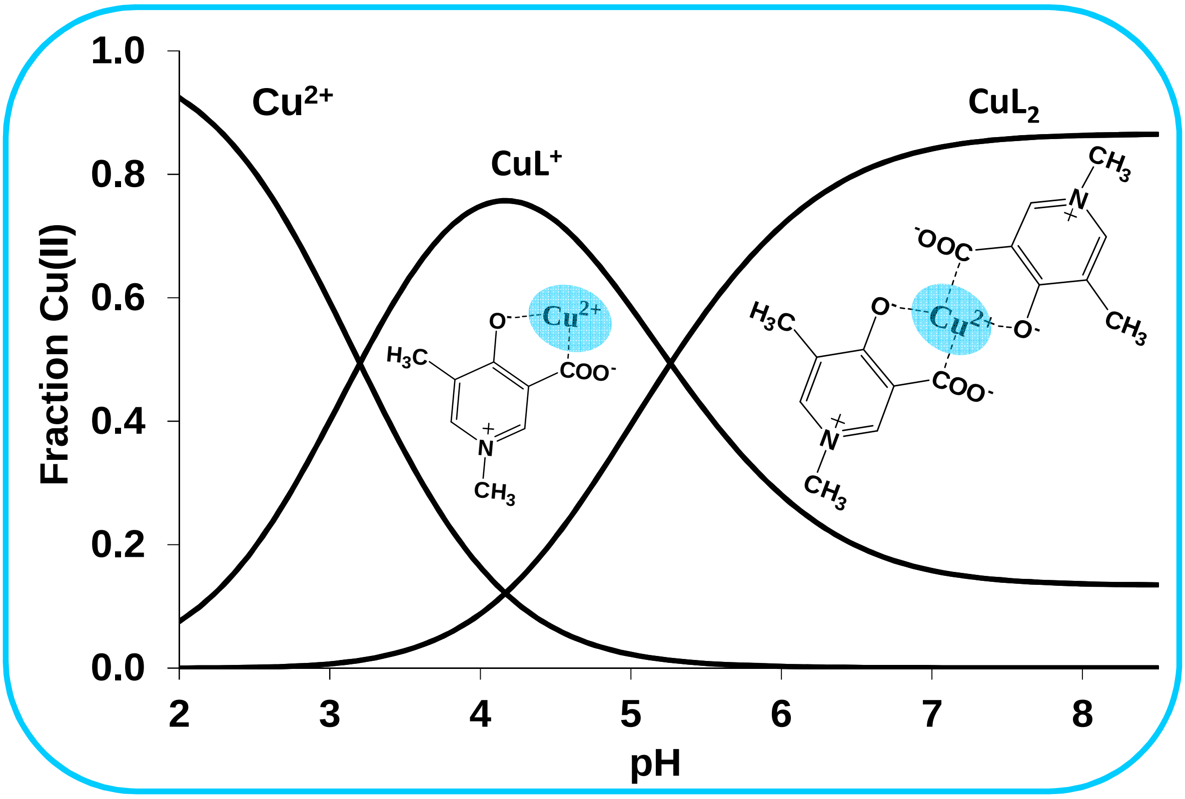

**Keywords**

Cu(II) and Zn(II) complex, carboxylate ligands, potentiometry, MTT-test, chelation therapy, neurodegenerative diseases

## 1. Introduction

Many transition metal ions, such a copper, iron and zinc, are essential for all living organisms. It is estimated that more than one-third of enzymes contain metal ions [1]. Furthermore they participate in a wide variety of biochemical processes in the cells. The equilibrium distribution of metal ions is crucial for many physiological functions.

Homeostasis of metal ions is critical for life and is maintained within strict limits [2]. In particular the redox active metals likely play a major role in altered redox balance. These metals, especially iron and copper, can undergo redox cycling and cause oxidative stress by increasing the formation of reactive oxygen species (ROS) as superoxide ion, hydrogen peroxide, and hydroxyl radical, resulting in the damage of many biomolecules in the cells.

Copper (Cu) is an essential trace metal used as a catalytic cofactor for many enzymes [3,4,5]. Copper ion exists in Cu(I) and Cu(II) oxidation states and can undergo electron transfer reactions in living systems in a similar way as for Fe(III)/Fe(II). In the reductive environment of the cell, Cu(II) can be reduced to Cu(I) by ascorbate or glutathione, and the reduced copper(I) can be oxidised to Cu(II) through the Fenton-type reaction[6,7]. The reduced metal ions such as Fe(II) and Cu(I) generate extremely reactive hydroxyl radicals from hydrogen peroxide in $\mathrm{M(red)} + \mathrm{H_2O_2} \rightarrow \mathrm{M(ox)} + \mathrm{OH}^{\bullet} + \mathrm{OH}^{-}$ reaction [6,7]. Copper excess or deficiency can cause impaired cellular functions and eventually cell death [3]. Copper deficiency causes impaired energy production, abnormal glucose and cholesterol metabolism, increased oxidative damage, increased tissue iron (Fe), altered structure and function of circulating blood and immune cells, abnormal neuropeptide synthesis and processing, aberrant cardiac electrophysiology, impaired myocardial contractility, and persistent effects on neurobehavior and on the immune system [8,9,10]. Nowadays it appears that the copper excess causes even more significant health problems. Some scientists believe that environmental factors are responsible for the increased copper uptake. The metal ion might be more bioavailable because it is leached from copper plumbing in homes or ingested as inorganic copper from vitamin/mineral supplements [16]. Cu overload is implicated in the pathogenesis of a variety of human diseases like cancer, cirrhosis, atherogenesis and neurodegenerative diseases [5]. Copper can also play a key role in the copper metabolism disorders as Menkes [11] and Wilson [12] diseases, and neurodegenerative disorders like familial amyotrophic lateral sclerosis or prion diseases [13]. Several studies indicate that the homeostasis of Cu(II) may become abnormal with aging. The copper level in the plasma is higher when compared to reference values obtained from healthy adults [14,15]. Many mechanisms have been demonstrated to influence the Alzheimer disease (AD), and they evidence that copper has a dramatic influence in the development of AD [16] and plays critical roles in the β-amyloid plaque formation in the Alzheimer's brain. The interaction of copper with amyloid precursor protein or Aβ-peptide (Aβ) can produce neurotoxic $H_2O_2$ (through the reduction of Cu(II)) and lead to oxidative stress in brain [17,18,19]. Some selective ligands for Cu(II) have been proposed as chelating agents for the therapy of AD. The first was clioquinol (CQ), which could chemically solubilize Aβ deposits in AD [20] likely through the interaction with copper. Faller and coworkers suggested that a chelator with a conditional dissociation constant ($K_D$) of 1 pM for Cu(II) should be sufficient to retrieve copper completely from amyloid deposits [21]. Other results show that an αB-crystallin chaperon peptide prevents Cu(II)-induced aggregation of $A\beta_{1-40}$ due to selective Cu(II) binding ability in addition to preventing the amyloid fibril formation of Aβ peptides [22]. The dissociation constant ($K_D$) for Cu(II) interaction with the chaperon peptide is in the μmol/$dm^3$ range [22,23].

Zn is an essential and redox inert trace element. Its role in the neurodegenerative processes is not completely evidenced. Reported Zn(II) affinity for Aβ is significantly weaker than, that for Cu(II), values of dissociation constants ranging between 1 and 20 μmol/$dm^3$ [21]. However, the amyloid aggregates contain relatively high concentration (mmol/$dm^3$) of zinc [24]. Several attempts were made to obtain efficient chelators with moderate affinity towards the metal ions such as Cu(II), Zn(II) or Fe(III) that participate of the amyloid aggregation, in order to prevent the formation of plaques [27].

In previous papers [28,36,37,42-44] we reported the evaluation of some hydroxypyridinecarboxylic acid derivatives (HPCs) as possible chelating agents for iron (Fe) and aluminium (Al(III)). To this aim, the Fe(III) and Al(III) complexes formed by selected HPCs were studied. Now we extended these studies also to Cu(II) and Zn(II). On one side, it is well known that any Fe(III) and Al(III) chelator can complex also essential metal ions in a chelation therapy regiment, thus causing toxic side effects due to metal ion deficiency. For example, zinc deficiency problems are sometimes experienced in the deferiprone therapy [25,26]. The evaluation of the complexation strength of HPCs towards Cu(II) and Zn(II) can allow to predict the extent of essential metal ion removal during the Fe(III) and Al(III) chelation therapy. On the other side, the very low cytotoxicity of HPCs and their low molecular weight (which can allow the oral activity and the blood brain barrier crossing) can represent important advantages also for the employment of HPCs in the AD therapy. Therefore, the evaluation of the complexation strength of the HPCs towards Cu(II) and Zn(II) can allow to predict if these ligands can remove copper and zinc from Aβ, *i.e.*, if they represent good candidates also in the recovery of the disturbed brain metal ion homeostasis on AD.

In the present paper we studied the Cu(II) and Zn(II) binding affinity of two HPCs derivatives: 4-hydroxy-5-methyl-3-pyridinecarboxylic acid (DQ5) and 1,5-dimethyl-4-hydroxy-3-pyridinecarboxylic acid (DQ715) (Scheme 1). Their coordination properties in aqueous solution were determined by means of pH-potentiometric titrations, UV-vis and

$^1H$ NMR or EPR measurements. The effects of DQ715 with Cu(II) chloride were evaluated on cell viability of a combined way in human embryonic kidney HEK-293 cells.

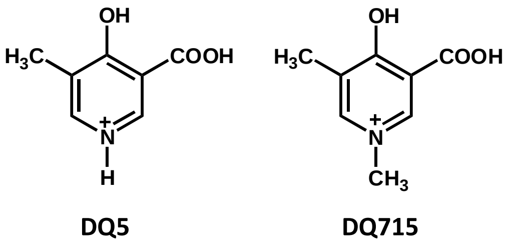

**Scheme 1.** 4-hydroxy-5-methyl-3-pyridinecarboxylic acid (DQ5) and 1,5-dimethyl-4-hydroxy-3-pyridinecarboxylic acid (DQ715) shown in their fully protonated forms ($H_3L^+$ and $H_2L^+$, respectively)

## 2. Experimental

**Chemicals:** DQ5 and DQ715 were synthesized as described in Ref [28]. Double-distilled Milli-Q water was used for sample preparations. The purity of the ligands was checked and the exact concentrations of the stock solutions prepared were determined by potentiometric titrations using the program SUPERQUAD for data evaluation [29]. The pH-metric titrations were performed with 0.1 mol/dm$^3$ KOH prepared from KOH (Merck). The base was standardised against HCl solutions prepared from 36% HCl (Merck). A $ZnCl_2$ stock solution was made by dissolution of anhydrous $ZnCl_2$ in a known amount of HCl, and its concentration was determined by complexometry via ethylenediaminetetraacetate complexes, and gravimetrically via the oxinate. The $CuCl_2$ ion stock solutions were prepared from $CuCl_2 \cdot 2H_2O$ (Reanal) dissolved in doubly distilled water, and the concentration of the metal ion was determined gravimetrically via precipitation of the oxinate.

**pH-potentiometric studies:** the pH-metric measurements for determining stability constants of the proton and metal complexes of the ligands were carried out at an ionic strength of 0.2 mol/dm$^3$ KCl (Sigma Aldrich) at 25.0 ± 0.1°C in aqueous solution. The titrations were performed with a carbonate-free KOH solution of know concentration (ca. 0.1 mol/dm$^3$). In order to keep the ionic strength constants KCl has been added to the KOH solution to set the $K^+$-concentration 0.2 mol/dm$^3$. The HCl concentrations were determined by potentiometric titrations using Gran’s method [30]. An Orion 710A pH-meter equipped with a Metrohm combined electrode (type 6.0234.1000) and a Metrohm 665 Dosimat burette was used for the pH-metric measurements. The electrode system was calibrated according to Irving *et al.* [34] (strong acid vs. strong base; HCl vs. KOH titration) and therefore the pH-meter readings could be converted into hydrogen ion concentration. The water ionization constant, p$K_w$ calculated from strong acid-strong base titrations was 13.76 ± 0.01 under the conditions employed. The titrations were performed in the pH range 2 – 11 or until precipitation occurred in the samples. The initial volume of the samples was 10 cm$^3$ in case of DQ715 and 20 cm$^3$ in case of DQ5 related titrations. The ligand concentration was in the range of $0.5 \times 10^{-3} - 2 \times 10^{-3}$ mol/dm$^3$, and the metal ion to ligand ratios were 1:1, 1:2 and 1:4. The accepted fitting of the titration curves was always less than 0.01 cm$^3$ and the uncertainties (3SD values) in the stability constants are given in parentheses in Table 1. The samples were in all cases deoxygenated by bubbling purified argon for *ca*. 10 min before the measurements, and argon was also passed across the solutions during the titrations.

The protonation constants of the ligands were determined with the computer program SUPERQUAD [29]. PSEQUAD [31] was utilized to establish the stoichiometry of the complexes and to calculate their stability constants ($\log\beta(M_pL_qH_r)$. $\beta(M_pL_qH_r)$ is defined for the general equilibrium reaction $pM + qL + rH \rightleftharpoons M_pL_qH_r$ as $\beta(M_pL_qH_r) = [M_pL_qH_r]/[M]^p[L]^q[H]^r$, where M denotes the metal ion, L is the completely deprotonated ligand molecule, and $p$, $q$ and $r$ are the number of metal, ligand, and proton atoms, respectively. According to the calibration protocol employed, the protonation and stability constants are concentration constants which refer to the given ionic strenght. The calculations were always made from the experimental titration data measured in the absence of any precipitate in the solution.

**Spectrophotometric measurements:** UV-Vis spectrophotometric measurements were performed in aqueous solution at 25.0 ± 0.1 °C on solutions containing the ligand (either DQ715 or DQ5) at a $8.0 \times 10^{-5}$ mol/dm$^3$ concentration, and the metal (either Cu(II) or Zn(II)) at the following metal to ligands ratios: 0:1, 1:4, 1:2, 1:1. The pH range was from 2 to 11, and the ionic strength was 0.20 mol/dm$^3$ (KCl). The spectra were recorded under argon atmosphere. A Hewlett Packard 8452A diode array spectrophotometer was used to record the UV-vis spectra in the interval 290 – 820 nm. The pathlength was 1 cm using quartz cuvettes. Protonation and stability constants and the individual spectra of the species were calculated by the computer program PSEQUAD [31].

**$^1$H NMR measurements:** $^1$H NMR studies were carried out on a Bruker Ultrashield 500 Plus instrument equipped with a 5 mm capillary NMR tube. In the NMR measurements the magnetic field was stabilised by locking with the $^2$D signal of the solvent. The sample temperature was set to 25 ± 1 °C during all data acquisitions. Chemical shifts are reported in ppm ($\delta_H$) from 4,4-dimethyl-4-silapentane-1-sulfonic acid (DSS) as internal reference. The $^1$H NMR measurements were performed with a WATERGATE solvent suppression scheme. All samples were measured with the same experimental parameters, the same spectrometer and the same probe. The relaxation delay, the delay for binomial water suppression, and the number of scans, were respectively 2 s, 150 μs, and 64. Spectra were collected for DQ5 and DQ715 ligands and for Zn(II) – DQ715 system in 90:10 $H_2O/D_2O$ mixtures at 1.1 mmol/dm$^3$ (DQ5) and 2 mmol/dm$^3$ (DQ715) ligand concentration. The Zn(II) – DQ715 ratios were 0:1, 1:1, 1:2 and 1:4. The ionic strength was adjusted to I = 0.2 mol/dm$^3$ with KCl in each sample. The pH of the solutions ($pH_{observed}$) was measured with a pH-sensitive glass electrode (Metrohm 6.0234.100) and an Orion 710A pH meter, calibrated according to the procedure described in the literature [34]). The equilibrium constants and the limiting chemical shifts of the species formed during protonation and Zn(II)-complexation were calculated by PSEQUAD [31].

**EPR measurements:** All CW-EPR spectra were recorded with a BRUKER EleXsys E500 spectrometer (microwave frequency ~9.7 GHz, microwave power 13 mW, modulation amplitude 5 G, modulation frequency 100 kHz). The isotropic EPR spectra were recorded at room temperature in a circulating system during a titration. Nine EPR spectra were recorded at 1 mmol/dm$^3$ $CuCl_2$ and 2 mmol/dm$^3$ DQ715 ligand concentration, and six at 2 mmol/dm$^3$ $CuCl_2$ and 2 mmol/dm$^3$ DQ715 ligand concentration, in the pH range 2 – 6 and 2 – 8.5, respectively. At higher pH values precipitation was detected in both cases. The ionic strength of 0.2 mol/dm$^3$ were adjusted with KCl. KOH solution was added to the stock solution to change the pH which was measured with an Orion 710A pH-meter equipped with a Metrohm 6.0234.100 glass elecrode. A Heidolph Pumpdrive 5101 peristaltic pump was used to circulate the solution from the titration pot through a capillary tube into the cavity of the instrument. The titrations were carried out under nitrogen atmosphere. At various pH values, samples of 0.1 cm$^3$ were taken, and frozen in liquid nitrogen, and the CW-EPR spectra were recorded under the same instrumental conditions as the room-temperature spectra described above.

**Evaluation of EPR spectra:** The series of room-temperature EPR spectra were simulated simultaneously by the „two-dimensional" method using the 2D_EPR program [32]. Each component curve was described by the isotropic EPR parameters $g_o$, $A_o^{Cu}$ copper hyperfine coupling, and the relaxation parameters $\alpha$, $\beta$, $\gamma$ which define the linewidth through the equation $\sigma_{MI} = \alpha + \beta M_I + \gamma M_I^2$, where $M_I$ denotes the magnetic quantum number of copper nucleus. The concentrations of the complexes were varied by fitting their formation constants, $\beta(M_pL_qH_r)$ defined above, in the experimental description of pH-potentiometric studies.

The anisotropic spectra were analysed individually by the EPR program [33], which gives the anisotropic EPR parameters ($g_x, g_y, g_z, A_x^{Cu}, A_y^{Cu}, A_z^{Cu}$) and the orientation dependent linewidth parameters).

For each spectrum, the noise-corrected regression parameter (*R)* is derived from the average square deviation (SQD) between the experimental and the calculated intensities. For the series of spectra, the fit is characterized by the overall regression coefficient *R*, calculated from the overall average SQD. The details of the statistical analysis were published previously [32]. Since a natural $CuCl_2$ was used for the measurements, all spectra were calculated as the sum of the spectra of $^{63}$Cu and $^{65}$Cu weighted by their natural abundances. The copper coupling constants and the relaxation parameters were obtained in field units (Gauss = $10^{-4}$ T).

**Cell cultures and Cytotoxicity Assay** Human Embryonic Kidney 293 (HEK-293) cell line was obtained by ATCC, Rockville, MD. Cells were maintained in the logarithmic phase at 37 °C in a 5 % carbon dioxide atmosphere using the D-MEM medium (Euroclone) containing 10 % fetal calf serum (Euroclone, Milan, Italy), antibiotics (50 units$\cdot$cm$^{-3}$ penicillin and 50 µg$\cdot$cm$^{-3}$ streptomycin) and 2 mmol/dm$^3$ L-glutamine. The growth inhibitory effect toward HEK-293 cell line was evaluated by means of MTT (tetrazolium salt reduction) assay [35]. Briefly, $3\cdot10^3$ cells were seeded in 96-well microplates in growth medium (0.1 cm$^3$) and then incubated at 37 °C in a 5% carbon dioxide atmosphere. After 24 h, cells were treated with the compound to be studied at the appropriate concentration. Triplicate cultures were established for each treatment. After 24 h, each well was treated with 0.01 cm$^3$of a 5 mg cm$^{-3}$ MTT saline solution, and after following 5 h of incubation, 0.1 cm$^3$ of a sodium dodecylsulfate (SDS) solution in HCl (0.01 mol/dm$^3$) were added. After overnight incubation in the dark at 37 °C in a 5 % carbon dioxide atmosphere, the inhibition of cell growth induced by tested compounds was detected by measuring the absorbance of each well at 570 nm using a Bio-Rad 680 microplate reader (Milan, Italy). Mean absorbance for each drug dose was expressed as a percentage of the control untreated well absorbance and plotted *vs*. drug concentration. $IC_{50}$ values represent the drug concentrations that reduced the mean absorbance at 570 nm to 50 % of those in the untreated control wells.

## 3. Results and discussion

### 3.1. Protonation constants

The acid-base properties of DQ5 and DQ715 were studied by potentiometric and spectroscopic techniques. The protonation constants presented here for these ligands are in good agreement with those reported in previous papers, when the difference in ionic strength is taken into account [28]. The $pK_a$ values also corresponds to those of related compounds with different ring substituents [28,36,37,38].

The protonation constants of DQ715, and DQ5 are listed in Table 1. The significant decreases in acidity of the carboxylic group in the ligands (log $K(COO^-) \leq 1$) can be mainly attributed to the formation of an intramolecular hydrogen-bonding between the $COO^-$ and the phenolic OH, which favours the liberation of the first proton [28]. The significantly lower second $pK_a$ in DQ715 than the $pK_a$ of the phenolic OH in phenol molecule or in salicylic acid has presumably due to the possibility of the formation of a chinoid isomeric structure (Scheme 2). The existence of the chinoidic and aromatic isomer forms of $L^-$ is supported by $^1H$ NMR measurements (Fig. 1.a.).

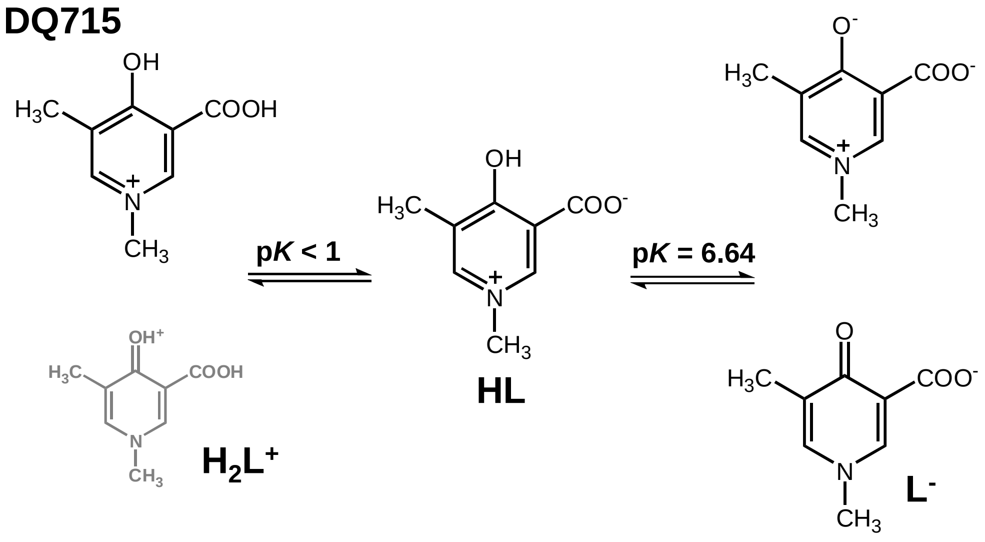

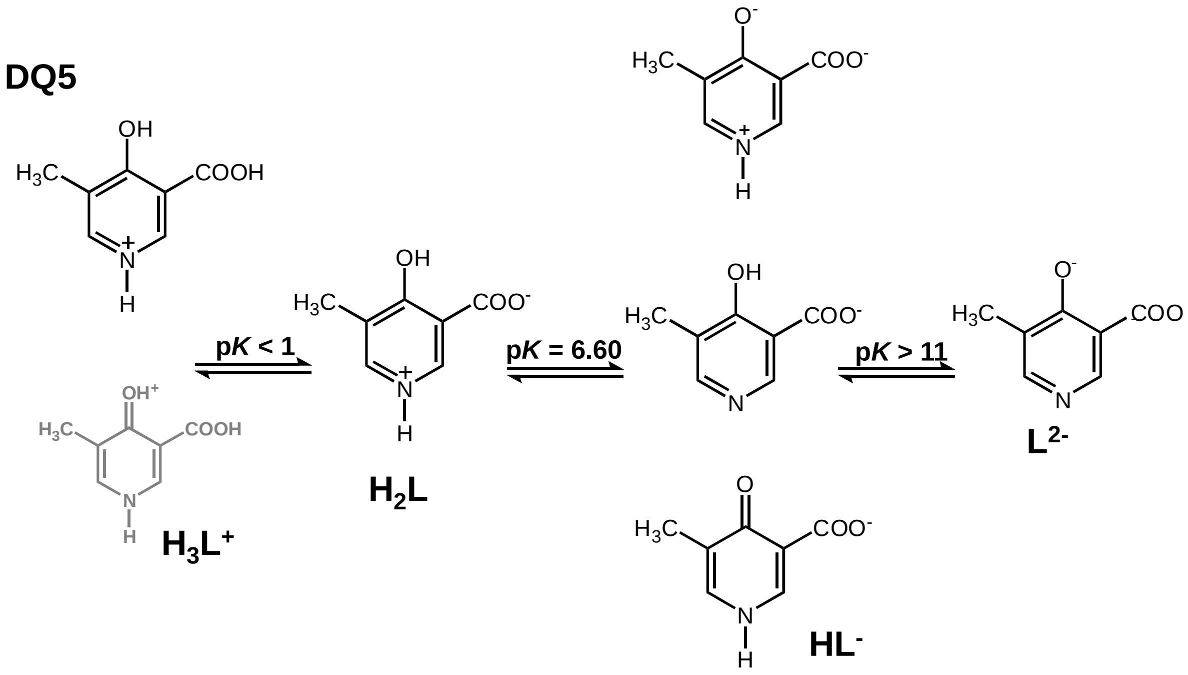
DQ5
pK < 1
pK = 6.60
pK > 11
H3L+
H2L
HL-
L2-

**Scheme 2.** Deprotonation steps of DQ5 and DQ715

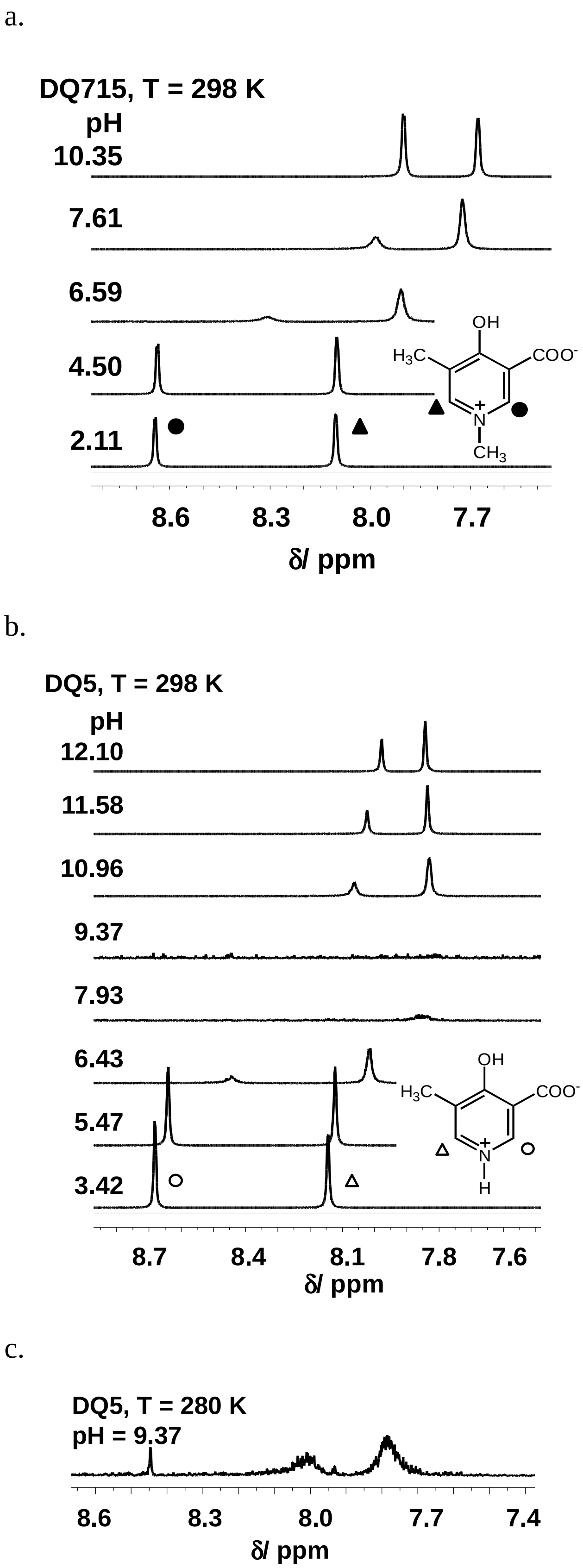

**Fig. 1.** Low-field region of the $^1$H NMR spectra of the ligands at the indicated pH values at $T$ = 298 K (a, b) and $T$ = 280 K (c) ($c_{DQ5}$ = $1.1 \times 10^{-3}$ mol/dm$^3$, $c_{DQ715}$ = $2 \times 10^{-3}$ mol/dm$^3$ $I$ = 0.2 mol/dm$^3$(KCl))

The exclusive formation of HL is seen at pH 2.11 and 4.50. Increasing the pH the signals start to broaden and shifted. The shifting can be explained by the deprotonation processes and the broadening may support the assumption that two tautomeric forms exist at these pH values. The chinoidic and the aromatic forms are in a fast exchange with respect to the $^1$H NMR time scale resulting in the broadened signals, however, at pH 10.35 the peaks become sharp again suggesting that a single species, the aromatic form is dominating again at this high pH.

An unequivocal assignment of the p$K_2$ and p$K_3$ values of DQ5 is not possible either, because 4-hydroxypyridine derivatives can adopt a chinoid electronic configuration in tautomeric equilibrium with the corresponding aromatic form. In case of DQ5 three $HL^-$ forms can exist (Scheme 2.). The similar behavior could also be seen in the spectra (Fig. 1.b). The signals start to broaden and shift above pH ~ 5.4, and they practically disappear at 9.37. Probably at this pH value the three different forms exist simultaneously also in fast exchange. Increasing the pH the signals become sharp again. At pH 9.37 $^1$H NMR spectrum was recorded at 280 K (Fig. 1.c) too showing that one of the signals ($\delta$ = 8.45 ppm) separated and became sharper while the signals of the other two isomers remained broad. This spectrum may also support the coexistence of three forms in the pH range 6.0 – 9.7.

The last p$K_a$ of DQ5 could not be accurately measured because it is too high. Therefore, we disregarded the last proton dissociation process and considered HL as the complex-forming species in the equilibrium $p\mathrm{M} + q\mathrm{HL} + r\mathrm{H} = \mathrm{M}_p\mathrm{L}_q\mathrm{H}_{r+q}$ (for simplicity, charges will be generally omitted from the formulae, except in the Tables). In this way, more accurate formation constants were obtained, although their numerical values differ by the value of the last p$K_a$ from those calculated in the usual way for the equilibrium $p\mathrm{M} + q\mathrm{L} + r\mathrm{H} = \mathrm{M}_p\mathrm{L}_q\mathrm{H}_r$.

Table 1. p$K_a$ values of DQ5 and DQ715, and stability constants of Cu(II) and Zn(II) complexes at 298 K in aqueous $I$ = 0.2 mol/dm$^3$(KCl)

| | **DQ5** | | **DQ715** | | | |
|---|---|---|---|---|---|---|
| species | p$K_a$ / log $\beta$ | | species | p$K_a$ / log $\beta$ | | |
| | pH-pot | UV-vis | | pH-pot | UV-vis | $^1$H NMR |
| $H_3L^+$ | | 0.23(6)* | $H_2L^+$ | | 0.40(1)* | |
| $H_2L$ | 6.60(1) | 6.61(2) | HL | 6.64(1) | 6.63(1) | 6.66(1) |
| $HL^-$ | > 11 | | | | | |
| | pH-pot | UV-vis | | pH-pot | UV-vis | EPR |
| $Cu(HL)^+$ | 6.24(1) | 6.39(3) | $CuL^+$ | 6.27(1) | 6.41(2) | 6.47(2) |
| $Cu(HL)_2$ | 11.33(5) | 11.33(9) | $CuL_2$ | 10.95(2) | 10.97(5) | 11.02(2) |
| $K_D$ | 3.1 × 10$^{-7}$ mol/dm$^3$ | | 5.1 × 10$^{-7}$ mol/dm$^3$ | | | |
| | pH -pot | | | pH-pot | | $^1$H NMR |
| $Zn(HL)^+$ | 3.75(2) | | $ZnL^+$ | 3.77(2) | | 3.79(3) |
| $Zn(HL)_2$ | 6.9(1) | | $ZnL_2$ | 7.06(3) | | 6.96(7) |
| $K_D$ | 7.5 × 10$^{-4}$ mol/dm$^3$ | | 8.2 × 10$^{-4}$ mol/dm$^3$ | | | |

$K_D$ =$[M]_{free}$ $\Sigma[H_xL]/\Sigma[M_pH_qL_r]$ computed at pH 7.4 for $c_M$ = 2.5 ×10$^{-5}$ mol/dm$^3$, $c_L$ = 5.0 × 10$^{-5}$ mol/dm$^3$

* Data are taken from Ref [28]

### 3.2. Cu(II) – DQ5 and Cu(II) – DQ715 systems

The chelating ability of DQ5 and DQ715 for Cu(II) was evaluated on the basis of the cumulative formation constants of their complexes, which were determined by potentiometric, UV-vis, and (in case of DQ715) by EPR measurements.

The pH-potentiometric titration curves measured at 1:1, 1:2 and 1:4 metal ion-to-ligand concentration ratios, normalized to the ligand concentration, are depicted in Fig. 2. (In all cases, strong acid was added to the solution before titration in order to ensure acidic conditions at the beginning of the measurement. The amount of potassium hydroxide consumed by the strong acid has been subtracted from the total $OH^-$ consumption in Fig. 2.) The predominant species for both ligands are mono and bis comlexes. No other species could be assumed to improve the fit of the titration curves; e.g. no tris complex formation in measurable concentration could be indication under the experimental conditions.

The shape of the analogous titration curves in both Cu(II)–ligand systems are similar until pH 5, indicating similar processes in the solution. Significant differences between DQ5 and DQ715 are evident in slightly acidic and neutral solutions. Complex formation starts at $pH > 3$. After a proton loss at the carboxylic group, in the presence of the metal ion one deprotonation step is observed on the titration curves. Although potentiometric data do not give any structural information, it is reasonable that in all complexes the ligands coordinate to the metal ion through the carboxylate oxygen and phenolate (bidentate chelation), and the pyridine-N remains protonated in the Cu–DQ5 complexes in the pH range studied. This result is similar to those obtained for the complexes formed by 3-hydroxy-2-pyridinecarboxylic acid and 4-hydroxy-3-pyridinecarboxylic acid with aluminium(III) and iron(III) where the pyridine-N remains protonated in the complex at neutral pH [42].

The sharp break on the titration curve at ligand excess indicates that precipitation occurs at $pH \approx 5$ in the Cu(II)–DQ5 solutions. Although the precipitate was not accurately analysed, presumably it is the neutral bis complex $CuL_2$, as when the complex as filtered off and redissolved in dilute HCl acid, significant amount of the ligand could be detected spectrophotometrically. It should also be mentioned that in the samples with ligand excess precipitation started at the same metal ion concentration when the concentration of $CuL_2$ (as calculated from the stability constants listed in Table 1.) reached the value of about $2.7 \times 10^{-4}$ mol/dm$^3$.

a. Cu(II)–DQ5

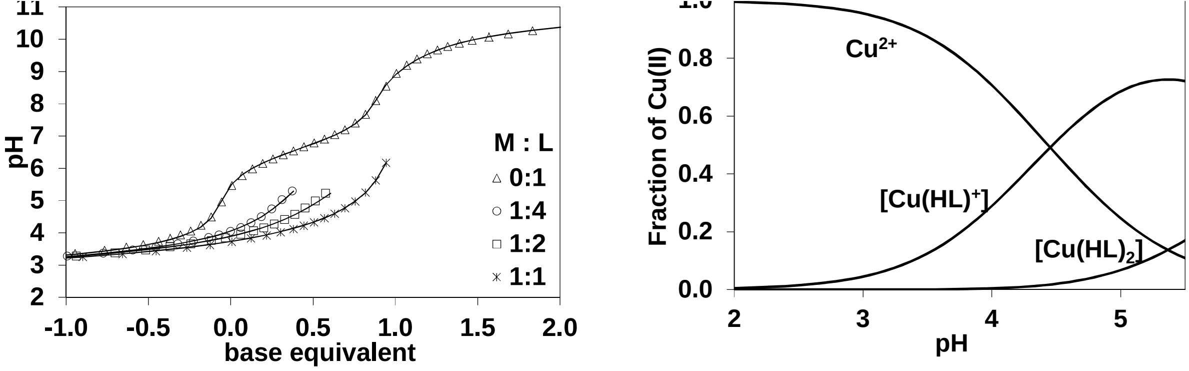

b. Cu(II)–DQ715

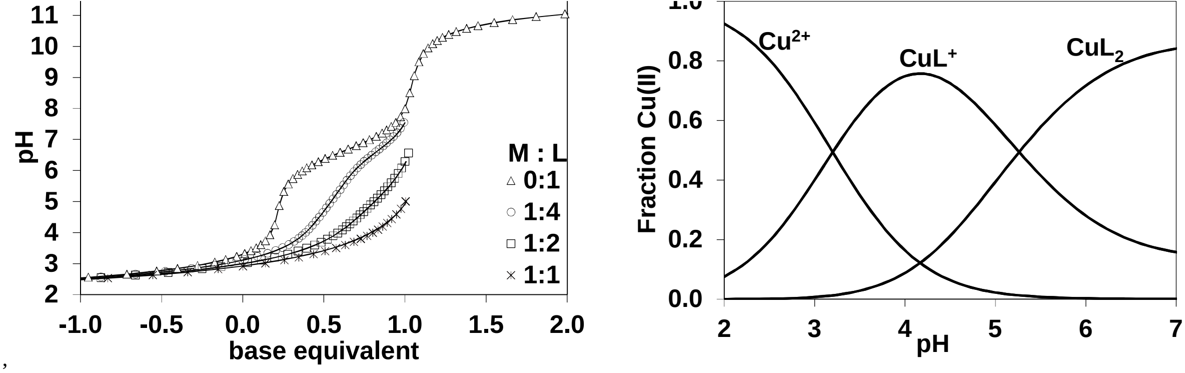

**Fig. 2.** Left: pH-potentiometric titration curves with the fitted curves (with continuous line) for ligands and for the copper(II)–ligands systems at different metal-to-ligand concentration ratios. Right: distribution diagrams of the most important Cu(II) species in the presence of:
(a) DQ5; $c_{Cu(II)} = 5 \times 10^{-4}$ mol/dm$^3$, $c_{DQ5} = 1 \times 10^{-3}$ mol/dm$^3$
(b) DQ715; $c_{Cu(II)} = 1 \times 10^{-3}$ mol/dm$^3$, $c_{DQ715} = 2 \times 10^{-3}$ mol/dm$^3$
($I = 0.2$ mol/dm$^3$ (KCl), $T = 298$ K)

Note that in the case of DQ5 the monoprotonated species while in the case of DQ715 the fully deprotonated catecholic L is the complex forming ligand form.

The limited solubility of the ligands in water allowed to carry out the pH-potentiometric titrations at a maximum of ~2 mmol×dm$^{-3}$ DQ715 and ~1 mmol×dm$^{-3}$ DQ5 concentrations, and despite the low solubility of DQ5 bis complex, interpretation of the potentiometric data leaves little doubt on the speciation model. We performed UV-vis spectrophotometric measurements to confirm the pH-potentiometric speciation result. Absorbance curves of the Cu(II)-DQ715 system are shown in Fig. 3.

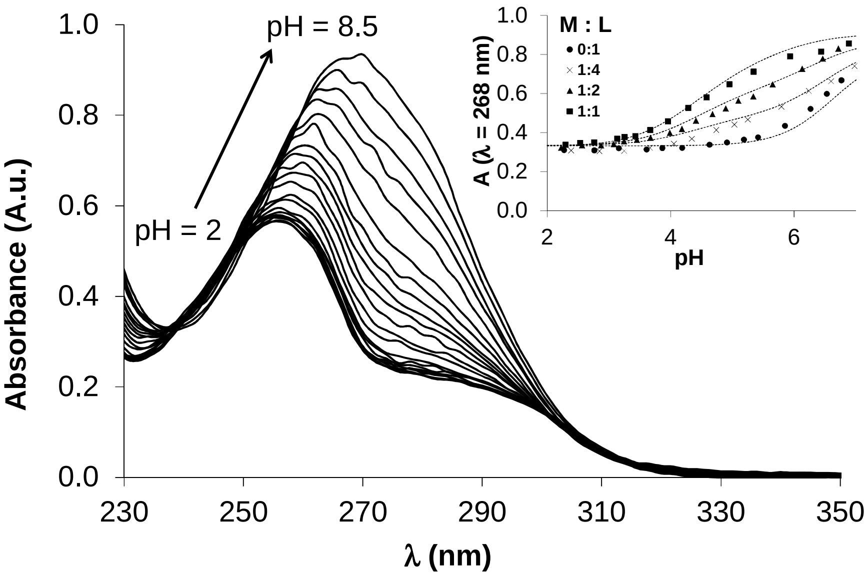

**Fig. 3.** Spectrophotometric absorbance curves of the Cu(II)–DQ715 system at various pH values; $c_{Cu(II)} = 4 \times 10^{-5}$ mol/dm$^3$, $c_{DQ715} = 8 \times 10^{-5}$ mol/dm$^3$. The inset shows the change in the absorbance the fitted curves were calculated (with dashed line) at 268 nm as function of the pH ($I = 0.2$ mol/dm$^3$ (KCl), $T = 298$ K)

Fig. 3. shows the pH-dependent UV-vis spectra of Cu(II)–DQ715 system and the change in the absorbance at 264 nm as function of the pH at various metal-to-ligand ratios. Spectra are very similar to those obtained for Cu(II)–DQ5 system (not shown). For DQ715 at pH 2, the main peak at 252 nm is due to $\pi \rightarrow \pi^*$ transition of the pyridinic ring, and by increasing the pH the deprotonation causes a bathochromic shift till around 270 nm. The presence of Cu(II) does not modify strongly the UV-vis spectra of the ligands. Only small modifications in the intensity and in the wavelength occur as a function of the pH. The complex formation was evidenced by monitoring of the absorption change in the wavelength range 230 – 350 nm. At in this low concentration no other absorption band disturbed the detected spectra. The stability constants of the different complexes/species were determined from the pH-dependent spectra. For both ligands, the UV-vis spectra allowed the detection of two complexes, CuL and $CuL_2$ for DQ715, and CuLH and $CuL_2H_2$ for DQ5 and the calculation of their stability constants. The UV-vis log $\beta$ values agree well with those determined by potentiometrically (see Table 1), thus confirming the formation of any other species in these metal-ligand systems.

EPR measurements were also carried out for Cu(II)–DQ715 solutions in order to obtain structural information on the complexes. The isotropic and anisotropic EPR spectra could be explained by taking into account the formation of CuL and $CuL_2$ complexes, beside the copper(II)aqua complex (Fig. 4). The slight decrease of the *g* values in CuL comparing with the $g$ values of the aqua complex indicates metal ion coordination by weak oxygen donors [$COO^{-}$,$O^{-}$]. Further decrease in $g$ and increase in $A$ values occur in $CuL_2$ indicating $2 \times$ [$COO^{-}$,$O^{-}$]coordination. The coordination of the two ligands in cis-trans geometric isomers could not be distinguished, possibly because of their very close EPR parameters. Determination of both isotropic and anisotropic EPR data of complexes CuL and $CuL_2$ allowed to predict the sign of their anisotropic copper hyperfine couplings ($A_x$ and $A_y$) (The determination of signs otherwise is a difficult problem and requires ENDOR or pulsed EPR measurements. The positive or negative sign of these two values can change easily because of the similar magnitudes but varying signs of the contributed Fermi contact term, spin-dipolar coupling and the spin-orbit interaction). In this study the measured isotropic hyperfine values have been compared with those of the averaged values calculated by the equation $A_o = (A_x + A_y + A_z)/3$ using different signs for $A_x$ and $A_{y.}$ (Negative sign for $A_z$ is known for copper(II) complexes with elongated octahedral geometry). The signs giving the best accordance are shown in Table 2. The good agreement between the measured and calculated values presume also that the complex structure formed in solution is kept upon freezing. Comparing the EPR parameters of CuL ($g_o$ = 2.166 and $A_o$ = 53 G) with those of copper(II)-fluorosalicylic acid analogoues ($g_o = \sim 2.179 – 2.186$ and $A_o = \sim 35 – 38$ G) [41], we can conclude that much higher $g_o$ values and lower $A_o$ values could be detected than for the different fluorosalicylic complexes. This indicates a significantly higher ligand field for DQ715 as compared to fluorosalicylic acid, owing to the positive inductive effect of the pyridinic nitrogen in contrast with the negative inductive effect of the fluorine. This agrees with the higher formation constants and the predominant formation of CuL in case of DQ715.

The formation constants and EPR parameters for the various Cu(II) complexes are summarized in Tables 1 and 2.

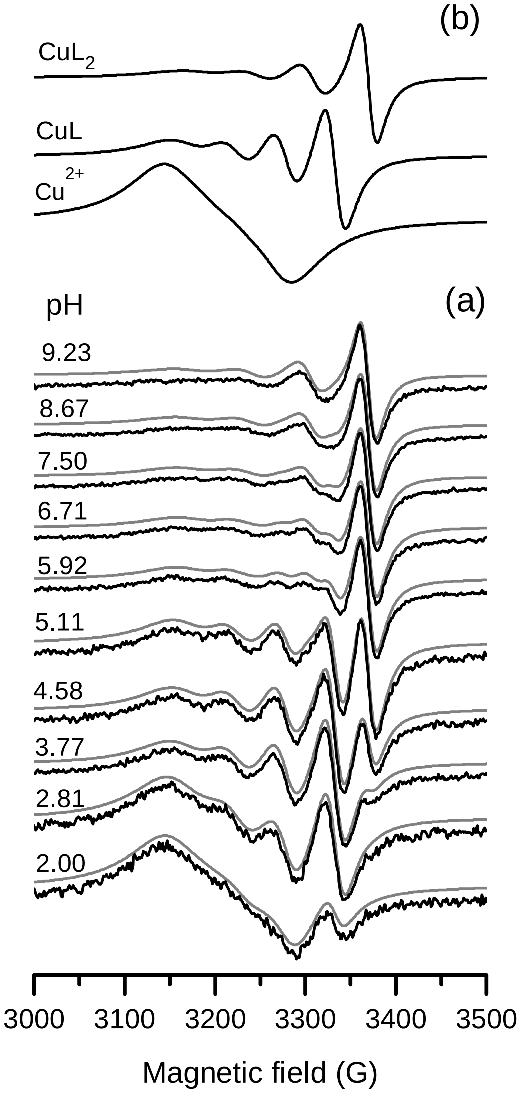

**Fig. 4.** (a) pH dependent series of experimental (black) and simulated (gray) EPR spectra ($c_{DQ715} = 2 \times 10^{-3}$ mol/dm$^3$, $c_{Cu} = 1 \times 10^{-3}$ mol/dm$^3$, $I = 0.2$ mol/dm$^3$ (KCl) $T = 298$ K), and (b) calculated component EPR spectra obtained by the „two-dimensional" simulation

**Table 2.** EPR parameters of components formed in Cu(II) –DQ715 system

| | Isotropic EPR data[a] | | Anisotropic EPR data[b] | | | | Calculated isotropic EPR data | |
|---|---|---|---|---|---|---|---|---|
| | $g_o$ | $\lvert A_o \rvert$ /G | $g_\perp$<br>$g_x, g_y$ | $g_\parallel$<br>$g_z$ | $A_\perp/G$<br>$A_x$, $A_y$ /$G^c$ | $A_\parallel/G$<br>$A_z$ / G | $g_{o,calc}$ | $\lvert A_{o,calc} \rvert^d$ /G |
| $Cu^{2+}$ | 2.194(1) | 34.6(6) | 2.079 | 2.412 | 8.0 | –116.0 | 2.190 | 37.5 |
| CuL | 2.166 (1) | 53.1(1) | 2.069, 2.069 | 2.347 | 12.0,<br>–12.0 | –147.0 | 2.161 | 53.2 |
| $CuL_2$ | 2.149 (1) | 60.8(1) | 2.066, 2.059 | 2.329 | –8.1,<br>–15.9 | –150.4 | 2.151 | 62.0 |

[a] Uncertainties (standard deviations) of the last digits are shown in parentheses. For the proton complexes the pH-potentiometric formation constants log$\beta$($LH_2$) = 7.66 and log$\beta$(LH) = 6.66 were used in the EPR analysis.

[b] The experimental errors were ± 0.001 for $g_x$ and $g_y$ and ± 0.0005 for $g_z$, ± 2 G for $A_x$ and $A_y$ and ± 1 G for $A_z$.

[c] The signs of the experimental values were derived from a comparison of $A_{o,calc}$ with the experimental $A_o$. [d] $\lvert A_{o,calc} \rvert = \lvert (A_x + A_y + A_z) / 3 \rvert$

### 3.3. Zn(II) – DQ5 and Zn(II) – DQ715 systems

The complex formation constants of Zn(II)–DQ715 and Zn(II)–DQ5 systems are listed in Table 1. Both systems comprise a small number of mononuclear complexes. The order of magnitude of the complex stability in this study are similar with the earlier findings in the Zn(II)–2-hydroxynicotinic acid system [44]. This suggests the same binding mode in these complexes, i.e. a bidentate coordination of the carboxylate and hydroxyl groups. Accordingly, the pyridine-N remains protonated in the complexes. Representative species-distribution diagrams for typical Zn(II)–DQ715 and Zn(II)–DQ5 solutions are shown in Fig. 5. The metal complex speciation in these systems do not differ considerably from each other. It can be seen that the complexation begins at pH 3.5 due to the formation of the monocomplex. The bis complex becomes predominant above pH 6. No evidence was found for the presence of any tris-complex. For both Zn(II)–DQ715 and Zn(II)–DQ5 systems, the pH interval which could be examined in potentiometric and $^1$H NMR measurements was limited because of the early precipitation of solid compounds. The pH at which the precipitation occurs (pH ≈ 8) and the appearance of the precipitate suggest that it is $Zn(OH)_2$.

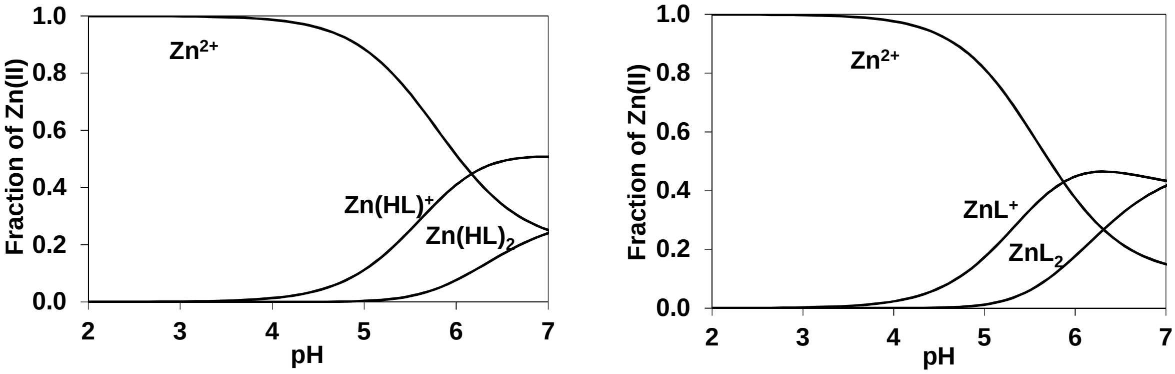

a. Zn(II)–DQ5

b. Zn(II)–DQ715

**Fig. 5.** Distribution diagrams of the most important Zn(II) species in the presence of
(a) DQ5; $c_{Zn(II)} = 5 \times 10^{-4}$ mol/dm$^3$, $c_{DQ5} = 1 \times 10^{-3}$ mol/dm$^3$
(b) DQ715; $c_{Zn(II)} = 1 \times 10^{-3}$, $c_{DQ715} = 2 \times 10^{-3}$ mol/dm$^3$
($I = 0.2$ mol/dm$^3$ (KCl) $T = 298$ K)

To support the potentiometric data, $^1$H NMR spectra were collected in the presence of DQ715 at various pH values in $H_2O/D_2O$ solution at 1:0, 1:1, 1:2, and 1:4 metal-to-ligand ratios. Due to the formation of the kinetically labile Zn(II) complexes, the position but not the number and multiplicity of the NMR signals, change as a function of pH. Stability constants of the complexes were calculated from the extent of shifts of the signals by PSEQUAD. Results are very similar to those obtained from the pH-potentiometry (Table 1). Fig. 6. shows the measured and calculated shifts of the N-CH-C-COO depending on the pH.

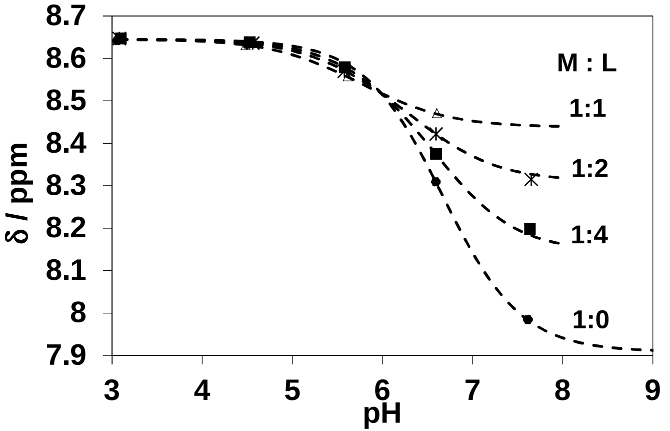

**Fig. 6.** Calculated and experimental $^1$H NMR shifts of the of N-CH-C-COO hydrogen of DQ715 as a function of the pH in Zn(II)–DQ715 system ($c_{DQ715} = 2 \times 10^{-3}$ mol/dm$^3$ $I = 0.2$ M (KCl) $T = 298$ K)

The Zn(II)–ligand complex formation was monitored by UV-vis spectrophotometric measurements too, but suitable UV-vis spectra could not be obtained because of the slight changes in the absorption due to the low level of complexes formation with both DQ5 and DQ715.

### 3.4. Cytotoxicity studies

HEK-293 human embryonic kidney cells were tested for their sensitivity to Cu(II) (as $CuCl_2$)-chloride and DQ715. Cells were treated for 24 h with increasing concentrations of $CuCl_2$ and DQ715, and cell viability was determined using the MTT test. Results are reported in Fig. 7.
As previously described [28], DQ715 proved to be hardly effective in decreasing cell viability, with an $IC_{50}$ value of 1.4 mmol×dm$^3$. Conversely, $IC_{50}$ calculated with $CuCl_2$ was 0.15 mmol×dm$^3$.

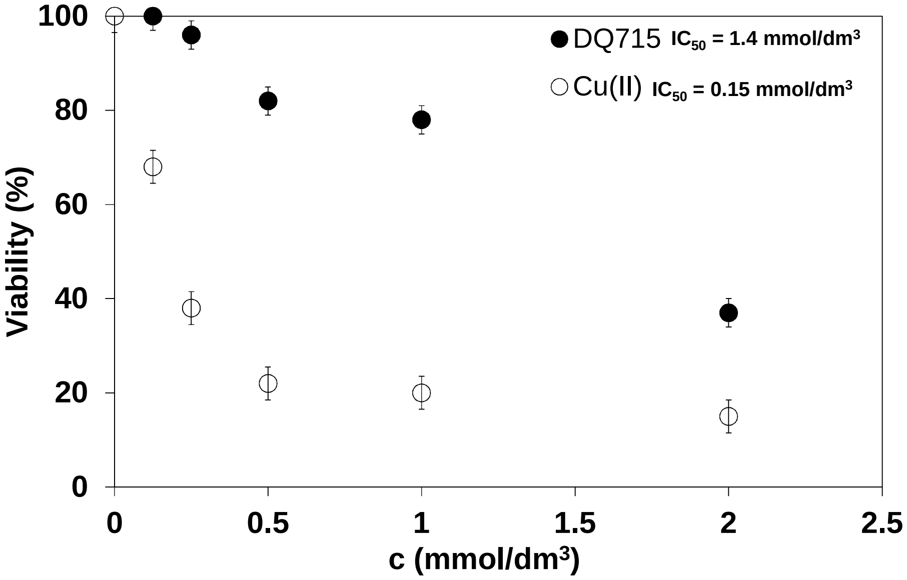

**Fig. 7.** Cytotoxicity profile of $CuCl_2$ and DQ715. HEK-293 cells were treated for 24 h with increasing concentrations of $CuCl_2$ (●) or DQ715 (○). Cytotoxicity was evaluated by the MTT test. $IC_{50}$ values were calculated by four parameter logistic model ($P < 0.05$). Values are shown as the means (±SD) of five independent experiments.

In order to study the effect of DQ715 in Cu(II) overload, HEK-293 cells were pre-treated with 0.15 mmol/dm$^3$ $CuCl_2$ for 24 h and further challenged with increasing concentrations (0.0 – 0.7 mmol/dm$^3$) of DQ715 for additional 24 h treatment. Fig. 8 shows the results obtained with MTT test. Co-treatment of HEK-293 cell with DQ715 and $CuCl_2$ determined a DQ715 dose-dependent decrease of copper salt cytotoxicity, supporting the hypothesis that DQ715 can reduce the cupper induced antiproliferative effect.

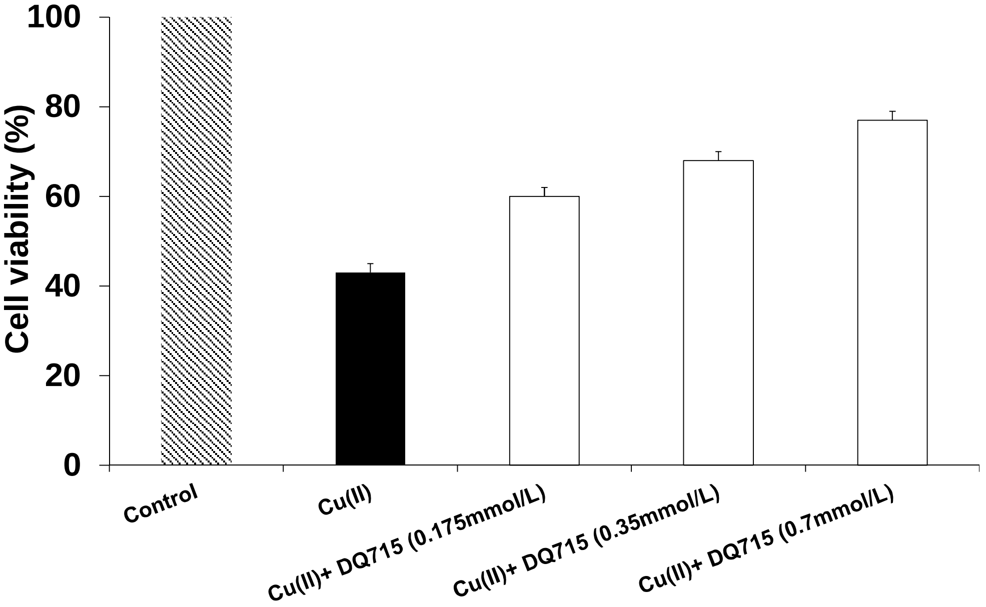

**Fig. 8.** Effect of Cu(II) and DQ715 combined treatment. HEK-293 cells were treated for 24 h with 0.15 mmol/dm$^3$ of $CuCl_2$ and then washed twice with PBS, and re-incubated with fresh complete medium (black) or medium added with increasing concentration of DQ715 (white), for further 24 h before MTT determination. Values are shown as the means (±SD) of five independent experiments.

## 4. Conclusions

The chemical interactions between the metals Zn(II) and Cu(II) and the ligands DQ715 and DQ5 have been investigated. The speciations are very similar, as only mononuclear mono and bis complexes are detected in solution. The two ligands have a similar metal binding ability towards Zn(II) and Cu(II). They are typical hard ligands and therefore form weaker Zn(II) and Cu(II) complexes than Fe(III) and Al(III) [28]. DQ715 forms slightly weaker complexes than DQ5 due to the N-methyl substitution of the pyridine ring which increases the hard character of the chelator. To compare the metal binding strength of the ligands at physiological pH, the $K_D$ values have been calculated for the complexes at pH 7.4. Values obtained are shown in Table 1. The order of magnitude of the $K_D$ value of the Zn(II) complexes is mmol/dm$^3$, that means that Zn(II) binding affinity of both ligands is very low. Therefore the ligands do not have any effect on the zinc homeostasis in vivo, i.e. DQ5 and DQ715 are expected to remove only a small amount of zinc. This low affinity may be important if DQ5 and DQ715 are used as Fe or Al chelators, because zinc deficiency problems are sometimes experienced in hard metal chelation therapy (e.g. for deferiprone [25,26]). DQ5 and DQ715 are expected to cause no zinc deficiency problem.

The affinity of the ligands for Cu(II) is higher than for Zn(II). The $K_D$ values are several tenth of micromolar for both ligands. The $K_D$ values reported in the literature for Cu(Aβ) range from 10 pM to 100 nM [21]. In any case it appears that DQ5 and DQ715 cannot retrieve Cu(II) from the amyloid-aggregates. However, the strength of the interactions with Cu(II) can be enough to bind the copper excess in the cells and protect them from the copper-induced redox processes, which would generate ROS species. This protection might explain why the Cu(II)-treated cells showed higher viability in the presence of DQ715. This protecting effect has been evaluated also in the presence of Fe(III), and in that case it was attributed to the metal chelation [28]. The acute and chronic Cu(II) toxicity can result in Cu(II)-induced oxidative damage that has been implicated in disorders associated with abnormal copper metabolism, liver disease and severe neurological defects. Therefore, although the ligand is not a suitable chelator for Cu(II) and cannot remove this ion from the beta-amyloid proteins, it appears suitable to protect the cells from the Fe(III) and Cu(II) related oxidative stress, which may be involved in neurodegenerative disorders, like Alzheimer's disease.

## Acknowledgements

This work was supported by the Hungarian Research Fund (OTKA K77833), and TÁMOP-4.2.2.A-11/1/KONV-2012-0052, supported by the European Union, and it was co-financed by the European Regional Fund and by the Italian-Hungarian CNR-HAS Bilateral Research Program "Venzo-Kiss". This research was realized in the frames of TÁMOP 4.2.4. A/2-11-1-2012-0001 „National Excellence Program – Elaborating and operating an inland student and researcher personal support system" The project was subsidized by the European Union and co-financed by the European Social Fund. T. Jakusch gratefully acknowledges the financial support of J. Bolyai research fellowship.

## References

[1] F.P. Guengerich, J. Biol. Chem., 284 (2009) 18557.

[2] I. Bertini, G. Cavallaro, J. Biol. Inorg. Chem., 13 (2008), 3.

[3] M. Arredondo, M.T. Núñez, Mol. Aspects Med., 26 (2005), 313.

[4] C. Fraga, Mol. Aspects Med., 26 (2005) 235.

[5] N. Arnal, M.J. Tacconi de Alaniz, C.A. Marra, Biochim. Biophys. Acta, 1820 (2012) 931.

[6] D.E. Carter, Environ. Health Perspect., 103 (1995) 17.

[7] K.T. Suzuki, T. Maitani, Biochem. J., 199 (1981) 289.

[8] E.D. Harris, Crit. Rev. Clin. Lab. Sci., 40 (2003) 547.

[9] C.L. Keen, L.A. Hanna, L. Lanoue, J.Y. Uriu-Adams, R.B. Rucker, M.S. Clegg, J. Nutr., 133 (2003) 1477S.

[10] J.T. Saari, Can. J. Physiol. Pharmacol., 78 (2000) 848.

[11] C. Vulpe, B. Levinson, S. Whitney, S. Packman, J. Gitschier, Nat. Genet., 3 (1993) 7.

[12] P.C. Bull, G.R. Thomas, J.M. Rommens, J.R. Forbes, D.W. Cox, Nat. Genet., 5 (1995) 327.

[13] E. Gaggelli, H. Kozłowski, D. Valensin, G. Valensin, Chem. Rev., 106 (2006) 1995 1995.

[14] A Schmuck, A.M Roussel, J Arnaud, V Ducros, A Favier, A Franco, J. Am. Coll. Nutr., 15 (1996) 462.

[15] A. Mezzetti, S.D. Pierdomenico, F. Costantini, F. Romano, D. De Cesare, F. Cuccurullo, T. Imbastaro, G. Riario-Sforza, F. Di Giacomo, G. Zuliani, R. Fellin Free Radical Biol. Med., 25 (1998) 676.

[16] G. J. Brewer, J. Trace Elem. Med. Bio., 26, (2012) 89.

[17] A.R. White, G. Multhaup, D. Galatis, W.J. McKinstry, M.W. Parker, R. Pipkorn, K. Beyreuther, C.L. Masters, R. Cappai, J. Neurosci., 22 (2002) 365.

[18] P.M. Doraiswamy, A.E. Finefrock, Lancet Neurol., 3 (2004) 431.

[19] J. Lu, D.M. Wu, Y.L. Zheng, D.X. Sun, B. Hu, Q. Shan, Z.F. Zhang, S.H. Fan, Brain, Behavior, and Immunity, 23 (2009) 193.

[20] R.A Cherny, J.T Legg, C.A McLean, D Fairlie, X Huang, C.S Atwood, K Beyreuther, R.E Tanzi, C.L Masters, A.I Bush, J. Biol. Chem., 274 (1999) 23223.

[21] P. Faller and C. Hureau, Dalton Trans., (2009) 1080.

[22] M.F. Ahmad, D. Singh, A. Taiyab, T. Ramakrishna, B. Raman, C.M. Rao, J. Mol. Biol., 382 (2008) 812.

[23] M. Raju, P. Santhoshkumar, T.M. Henzl, K.K. Sharma, Free Radical Biol. Med., 50 (2011) 1429.

[24] M.A. Lovell, J.D. Robertson, W.J. Teesdale, J.L. Campbell and W. R., Markesbery, J. Neurol. Sci., 158 (1998) 47.

[25] G.J. Kontoghiorghes, Toxicol. Lett. 80 (1995) 1.

[26] G.J. Kontoghiorghes, M.B. Agarwal, R.W. Grady, A. Koinagou,, J.J. Marx, Lancet 356 (2000) 428.

[27] H. Kozlowski, M. Luczkowski, M. Remelli, D. Valensin, Coord. Chem. Rev., 256 (2012) 2129.

[28] A. Dean, É. Sija, É. Zsigó, M. G. Ferlin, D. Marton, V. Gandin, C. Marzano, P.Pastore, D. Badocco, A. Venzoe, R. Bertani, T. Kiss, V. Di Marco, Eur. J. Inorg. Chem. 8 (2013) 1310-.

[29] P. Gans, A. Sabatini and A. Vacca, J. Chem. Soc., Dalton Trans., (1985) 1195.

[30] G. Gran, ActaChem. Scand., 4 (1950) 559.

[31] L. Zékány, I. Nagypál, D.L. Leggett (Ed.), Plenum Press, New York, 1985, 291.

[32] A. Rockenbauer, T. Szabó-Plánka, Zs. Árkosi, L. Korecz, J. Am. Chem. Soc. 123 (2001) 7646.

[33] A. Rockenbauer, L. Korecz, Appl. Magn. Reson. 10 (1996) 29.

[34] H.M. Irving, M.G. Miles, L.D. Petit, Anal. Chim. Acta, 38 (1967) 475.

[35] M.C. Alley, D.A. Scudiero, A. Monks, M.L. Hursey, M.J. Czerwinski, D.L. Fine, B.J. Abbott, J.G. Mayo, R.H. Shoemaker, M.R. Boyd, Cancer Res. 48 (1988) 589.

[36] E. Sija, A. Dean, T. Jakusch, V.B. Di Marco, A. Venzo, T. Kiss, Monatsh. Chem., 142 (2011) 399.

[37] A. Dean, M.G. Ferlin, P. Brun, I. Castagliuolo, R.A. Yokel, A. Venzo, G.G Bombi, V.B. Di Marco, Inorg. Chim. Acta, 373 (2011) 179.

[38] V.B. Di Marco, A. Dean, R.A. Yokel, H. Li, G.G. Bombi, Polyhedron, 26 (2007) 3227.

[39] A.E. Martell, R.M. Smith, Critical Stability Constants, Plenum, New York, vol. 2, 1975.

[40] M. Jezowska-Bojczuk, H. Kozlowski, A. Zubor, T. Kiss, M. Branca, G. Micera, A. Dessì, J. Chem. Soc., Dalton Trans. (1990) 2903.

[41] T. Szabó-Plánka, B. Gyurcsik, I. Pálinkó, N. V. Nagy, A. Rockenbauer, R. Šípoš, J. Šima, M. Melník, J. Inorg. Biochem 105 (2011) 75.

[42] V.B. Di Marco, R.A. Yokel, M.G. Ferlin, A. Tapparo, G.G. Bombi, Eur. J. Inorg. Chem. (2002) 2648.

[43] V.B. Di Marco, A. Tapparo, G.G. Bombi, Ann. Chim. (Rome), 89 (1999) 535.

[44] V.B. Di Marco, A.Tapparo, A. Dolmella, G.G. Bombi; Inorg.Chim. Acta 357 (2004) 135.

**Table 1.** p$K_a$ values of DQ5 and DQ715, and stability constants of Cu(II) and Zn(II) complexes at 298 K in aqueous $I$ = 0.2 mol/dm$^3$ (KCl)

| | **DQ5** | | **DQ715** | | | |
|---|---|---|---|---|---|---|
| species | p$K_a$ / log $\beta$ | | species | p$K_a$ / log $\beta$ | | |
| | pH-pot | UV-vis | | pH-pot | UV-vis | $^1$H NMR |
| $H_3L^+$ | | 0.23(6)* | $H_2L^+$ | | 0.40(1)* | |
| $H_2L$ | 6.60(1) | 6.61(2) | HL | 6.64(1) | 6.63(1) | 6.66(1) |
| $HL^-$ | > 11 | | | | | |
| | pH-pot | UV-vis | | pH-pot | UV-vis | EPR |
| $Cu(HL)^+$ | 6.24(1) | 6.39(3) | $CuL^+$ | 6.27(1) | 6.41(2) | 6.47(2) |
| $Cu(HL)_2$ | 11.33(5) | 11.33(9) | $CuL_2$ | 10.95(2) | 10.97(5) | 11.02(2) |
| $K_D$ | 3.1 × $10^{-7}$ mol/dm$^3$ | | 5.1 × $10^{-7}$ mol/dm$^3$ | | | |
| | pH -pot | | | pH-pot | | $^1$H NMR |
| $Zn(HL)^+$ | 3.75(2) | | $ZnL^+$ | 3.77(2) | | 3.79(3) |
| $Zn(HL)_2$ | 6.9(1) | | $ZnL_2$ | 7.06(3) | | 6.96(7) |
| $K_D$ | 7.5 × $10^{-4}$ mol/dm$^3$ | | 8.2 × $10^{-4}$ mol/dm$^3$ | | | |

$K_D$ =[M]$_{free}$ $\Sigma[H_xL]/\Sigma[M_pH_qL_r]$ computed at pH 7.4 for $c_M$ = 2.5 ×$10^{-5}$ mol/dm$^3$, $c_L$ = 5.0 × $10^{-5}$ mol/dm$^3$

* Data are taken from Ref [28]

**Table 2.** EPR parameters of components formed in Cu(II) –DQ715 system

| | Isotropic EPR data$^a$ | | Anisotropic EPR data$^b$ | | | | Calculated isotropic EPR data | |
|---|---|---|---|---|---|---|---|---|
| | $g_o$ | $\lvert A_o \rvert$ /$G$ | $g_\perp$ $g_x$,$g_y$ | $g_\parallel$ $g_z$ | $A_\perp$/$G$ $A_x$, $A_y$ /$G^c$ | $A_\parallel$/$G$ $A_z$ / $G$ | $g_{o,calc}$ | $\lvert A_{o,calc} \rvert^d$ /$G$ |
| $Cu^{2+}$ | 2.194(1) | 34.6(6) | 2.079 | 2.412 | 8.0 | -116.0 | 2.190 | 37.5 |
| CuL | 2.166 (1) | 53.1(1) | 2.069, 2.069 | 2.347 | 12.0,<br>-12.0 | -147.0 | 2.161 | 53.2 |
| $CuL_2$ | 2.149 (1) | 60.8(1) | 2.066, 2.059 | 2.329 | -8.1,<br>-15.9 | -150.4 | 2.151 | 62.0 |

[a] Uncertainties (standard deviations) of the last digits are shown in parentheses. For the proton complexes the pH-potentiometric formation constants log$\beta(LH_2)$ = 7.66 and log$\beta$(LH) = 6.66 were used in the EPR analysis.

[b] The experimental errors were ± 0.001 for $g_x$ and $g_y$ and ± 0.0005 for $g_z$, ± 2 G for $A_x$ and $A_y$ and ± 1 G for $A_z$.

[c] The signs of the experimental values were derived from a comparison of $A_{o,calc}$ with the experimental $A_o$.

[d] $\lvert A_{o,calc} \rvert = \lvert (A_x + A_y + A_z) / 3 \rvert$

## Legends to Figures

**Scheme 1.** 4-hydroxy-5-methyl-3-pyridinecarboxylic acid (DQ5) and 1,5-dimethyl-4-hydroxy-3-pyridinecarboxylic acid (DQ715) shown in their fully protonated forms ($H_3L^+$ and $H_2L^+$, respectively)

**Fig. 1.** Low-field region of the $^1H$ NMR spectra of the ligands at the indicated pH values at $T = 298$ K (a, b) and $T = 280$ K (c) ($c_{DQ5} = 1.1 \times 10^{-3}$ mol/dm$^3$, $c_{DQ715} = 2 \times 10^{-3}$ mol/dm$^3$ $I = 0.2$ mol/dm$^3$(KCl))

**Fig. 2.** Left: pH-potentiometric titration curves with the fitted curves (with continuous line) for ligands and for the copper(II)–ligands systems at different metal-to-ligand concentration ratios. Right: distribution diagrams of the most important Cu(II) species in the presence of:
(a) DQ5; $c_{Cu(II)} = 5 \times 10^{-4}$ mol/dm$^3$, $c_{DQ5} = 1 \times 10^{-3}$ mol/dm$^3$
(b) DQ715; $c_{Cu(II)} = 1 \times 10^{-3}$ mol/dm$^3$, $c_{DQ715} = 2 \times 10^{-3}$ mol/dm$^3$
($I = 0.2$ mol/dm$^3$ (KCl), $T = 298$ K)

**Fig. 3.** Spectrophotometric absorbance curves of the Cu(II) – DQ715 system at various pH values; $c_{Cu(II)} = 4\times10^{-5}$ mol/dm$^3$, $c_{DQ715} = 8\times10^{-5}$ mol/dm$^3$. The inset shows the change in the absorbance the fitted curves were calculated (with dashed line) at 268 nm as function of the pH ($I = 0.2$ mol/dm$^3$ (KCl), $T = 298$ K)

**Fig. 4.** (a) pH dependent series of experimental (black) and simulated (gray) EPR spectra ($c_{DQ715} = 2 \times 10^{-3}$ mol/dm$^3$, $c_{Cu} = 1 \times 10^{-3}$ mol/dm$^3$, $I = 0.2$ mol/dm$^3$ (KCl) $T = 298$ K), and (b) calculated component EPR spectra obtained by the „two-dimensional" simulation

**Fig. 5.** Distribution diagrams of the most important Zn(II) species in the presence of
(a) DQ5; $c_{Zn(II)} = 5 \times 10^{-4}$ mol/dm$^3$, $c_{DQ5} = 1 \times 10^{-3}$ mol/dm$^3$
(b) DQ715; $c_{Zn(II)} = 1 \times 10^{-3}$, $c_{DQ715} = 2 \times 10^{-3}$ mol/dm$^3$
($I = 0.2$ mol/dm$^3$ (KCl) $T = 298$ K)

**Fig. 6.** Calculated and experimental $^1$H NMR shifts of the of N-CH-C-COO hydrogen of DQ715 as a function of the pH in Zn(II)–DQ715 system ($c_{DQ715}$ = 2 × $10^{-3}$ mol/dm$^3$ $I$ = 0.2 M (KCl) $T$ = 298 K)

**Fig. 7.** Cytotoxicity profile of $CuCl_2$ and DQ715. HEK-293 cells were treated for 24 h with increasing concentrations of $CuCl_2$ (●) or DQ715 (○). Cytotoxicity was evaluated by the MTT test. $IC_{50}$ values were calculated by four parameter logistic model ($P < 0.05$). Values are shown as the means (±SD) of five independent experiments

**Fig. 8.** Effect of Cu(II) and DQ715 combined treatment. HEK-293 cells were treated for 24 h with 0.15 mmol/dm$^3$ of $CuCl_2$ and then washed twice with PBS, and re-incubated with fresh complete medium (black) or medium added with increasing concentration of DQ715 (white), for further 24 h before MTT determination. Values are shown as the means (±SD) of five independent experiments